The IL32/BAFF axis supports prosurvival dialogs in the lymphoma ecosystem and is disrupted by NIK inhibition

Salomé Decombis,[1,2,3] Antonin Papin,[1,2,3] Céline Bellanger,[1,2,3] Clara Sortais,[1,2,3,4] Christelle Dousset,[1,2,3,4] Yannick Le Bris,[1,2,3,5] Thiphanie Riveron,[1,2,3] Stéphanie Blandin,[6] Philippe Hulin,[6] Benoit Tessoulin,[1,2,3,4] Mathieu Rouel,[1,2,3] Steven Le Gouill,[1,2,3,4] Agnès Moreau-Aubry,[1,2,3] Catherine Pellat-Deceunynck[1,2,3] and David Chiron[1,2,3]

[1]Nantes Université, INSERM, CNRS, Université d'Angers, CRCI2NA; [2]L'Héma-NexT, i-Site NexT; [3]GDR3697 Micronit, CNRS; [4]Service d'Hématologie Clinique, Unité d'Investigation Clinique, CHU; [5]Service d'Hématologie Biologique, CHU and [6]SFR-Santé, INSERM UMS016, CNRS UMS 3556, FED 4202, Nantes Université, CHU, Nantes, France

Correspondence: D. Chiron
david.chiron@univ-nantes.fr

Received: August 11, 2021.
Accepted: February 9, 2022.
Prepublished: March 10, 2022.

https://doi.org/10.3324/haematol.2021.279800

Abstract

Aggressive B-cell malignancies, such as mantle cell lymphoma (MCL), are microenvironment-dependent tumors and a better understanding of the dialogs occurring in lymphoma-protective ecosystems will provide new perspectives to increase treatment efficiency. To identify novel molecular regulations, we performed a transcriptomic analysis based on the comparison of circulating MCL cells (n=77) *versus* MCL lymph nodes (n=107) together with RNA sequencing of malignant (n=8) *versus* normal B-cell (n=6) samples. This integrated analysis led to the discovery of microenvironment-dependent and tumor-specific secretion of interleukin-32 beta (IL32β), whose expression was confirmed *in situ* within MCL lymph nodes by multiplex immunohistochemistry. Using *ex vivo* models of primary MCL cells (n=23), we demonstrated that, through the secretion of IL32β, the tumor was able to polarize monocytes into specific MCL-associated macrophages, which in turn favor tumor survival. We highlighted that while IL32β-stimulated macrophages secreted several protumoral factors, they supported tumor survival through a soluble dialog, mostly driven by BAFF. Finally, we demonstrated the efficacy of selective NIK/alternative-NFκB inhibition to counteract microenvironment-dependent induction of IL32β and BAFF-dependent survival of MCL cells. These data uncovered the IL32β/BAFF axis as a previously undescribed pathway involved in lymphoma-associated macrophage polarization and tumor survival, which could be counteracted through selective NIK inhibition.

Introduction

Although for years most studies have focused on tumor cells, allowing the discovery of numerous key (epi)-genetic aberrations and oncogenic pathways, it is now widely accepted that ecosystem integration is also critical for the understanding of cancer progression. Evidence demonstrating that the tumor ecosystem plays a central role in tumoral expansion and treatment resistance has continued to accumulate since the emergence of the tumor microenvironment concept more than a century ago.[1] Indeed, the tumor ecosystem has shown multiple facets, from its critical role in cancer metabolism to the influence of mechanical constraints, not to mention the diversity of immune infiltrates.[2] A better understanding of the tumor microenvironment now supports the development of next-generation therapeutic strategies, such as rational targeted therapy combinations to bypass microenvironment-dependent resistance,[3] immune checkpoint inhibitors and bi-specific antibodies.[4]

Mantle cell lymphoma (MCL) is a rare and mostly incurable B-cell malignancy and strategies to overcome resistance and treat MCL relapses are an unmet medical need.[5] Over the past decades, most studies have focused on structural and functional genomic anomalies which have led to important discoveries regarding the molecular origin of MCL (e.g., t(11;14)), factors involved in the highly heterogeneous clinical course of this disease (e.g., *SOX11*, *TP53*, and *CDKN2A*),[6-8] as well as markers of drug resistance.[9-11] In contrast to intrinsic tumoral anomalies, the dialog between MCL and its tumor microenvironment was largely ignored. Nevertheless, we, and others, have suggested a dynamic dialog within lymph nodes, which are the primary zone of MCL expansion. MCL cells are able to shape their microenvironment,[12] whereas the latter is necessary to trigger cell cycle activation,[13] inhibition of apoptosis and drug

resistance[14] as well as activation of oncogenic pathways, such as nuclear factor kappa B (NFκB) and B-cell receptor (BCR) pathways.[15] These findings confirmed the need to consider the biology of the tumor microenvironment in MCL and encourage further studies to understand the complexity of its dialogs and the supporting molecular regulations.

Unlike other B-cell lymphomas, MCL is characterized, as promptly as at diagnosis, by early dissemination in virtually all patients, with a significant number of circulating lymphoma cells, mostly in the bone marrow and peripheral blood (PB).[16] This characteristic allows the comparison of tumor cells within several organs and the identification of regulations specifically induced in the lymphoid niches. To identify tumor microenvironment-dependent molecular regulations in MCL, we first performed a global unbiased transcriptomic analysis integrating samples from PB and lymph node (LN) tissue and cells from *ex vivo* models. Our analysis uncovered the microenvironment-dependent and tumor-specific expression of interleukin-32 (IL32), a soluble factor whose role in lymphomas is unknown. We showed that tumor-specific IL32 plays a major role in the corruption of the immune ecosystem that supports MCL survival and identified druggable therapeutic targets involved in these interplays.

Methods

Primary cell culture

MCL cells were obtained after informed consent from patients according to protocols approved by local institutional review boards (REFRACT-LYMA cohort; ethical approval GNEGS-2015-09-13[17]) and in accordance with the Declaration of Helsinki. The patients' characteristics are summarized in *Online Supplementary Table S1*. For comparison with normal naïve $CD5^+$ B cells (NBC), cord blood B cells were isolated and cultured using the same protocol. As previously described, MCL and NBC were cultured with growth factors (interleukin [IL]10: 50 ng/mL, B-cell activating factor [BAFF]: 50 ng/mL, insulin-like growth factor-1 [IGF1]: 10 ng/mL, IL6: 1 ng/mL) on adherent CD40L-expressing fibroblasts previously treated with mitomycin-C.[13] The ratio of adherent cells to MCL cells was 1:10.

PB was obtained from age-matched (>60 years) healthy donors. Monocytes were obtained by elutriation and T cells were separated using anti-human CD3 magnetic beads. M1 and M2-10 monocyte-derived macrophages (M ϕ) were generated *in vitro* as previously described.[12] Regarding Mϕ-32, monocytes were differentiated with CSF1 (M-CSF, 50 ng/mL, for 5 days) before activation with recombinant human (rh)IL32β (100 ng/mL, for 2 days).

Bioinformatics analysis

Gene expression profiling

Publicly available datasets for MCL cells in LN (n=107) or PB (n=77) were collected from the Gene Expression Omnibus database (GSE70910, GSE16455, GSE21452, GSE35426, GSE36000, GSE124931 and GSE95405) and analyzed as previously described.[14]

Full-length RNA-sequencing

$CD19^+CD5^+$ MCL cells from PB (n=4) and $CD19^+CD5^+$ B cells from cord blood (NBC, n=3) were cultured *ex vivo* on CD40L-expressing fibroblasts with growth factors for 7 days.[13] RNA was sequenced at baseline (day 0) and after 7 days of culture. "Tumor-specific" and "Shared with NBC" genes were determined by comparing the transcriptome of MCL cells with that of NBC. "Tumor-specific" genes were found to be upregulated in culture *ex vivo* and in LN *in vivo* but not in NBC samples.

3'seq-RNA profiling[18]

Briefly, raw counts were normalized and transformed and differential gene expression was assessed with the DESeq2 package in R. Similar results were obtained using the EdgeR package in R. Principal component analysis was performed by FactoMineR and factoextra packages. A hierarchical ascendant clustering was performed using Euclidean distances and the Ward.D2 method. Heatmaps were created using the ComplexHeatmap package.

All datasets were deposited in the Gene Expression Omnibus database (GSE179636 and GSE179766).

Multiplex immunohistochemistry

Formalin-fixed paraffin-embedded tissue sections were subjected to pretreatment involving antigen retrieval by heating in EDTA buffer at the beginning of the experiment and to a TR1 retrieval between each staining. Tissue sections were then stained for Cyclin D1, IL32, CD68 and CD3 with polymer enhancer and HRP 2-Step polymer and the buffer 1X Plus Amplification Diluent with Opal 570, 650, 520 and 690 for the detection of Cyclin D1, IL32, CD68 and CD3, respectively. We used DAPI (1:4000) to stain the nuclei. The experiment was conducted in an automated lmpath36. Images were acquired on a Nikon A1 RSi confocal fluorescence microscope with spectral module.

Additional methods are detailed in the *Online Supplementary Methods* section and *Online Supplementary Table S2*.

Results

Microenvironment-dependent IL32 expression in mantle cell lymphoma cells is tumor specific

We first analyzed differential gene expression between

unpaired MCL samples from LN (n=107) and PB (n=77): 6,887 genes were differentially expressed (log_2Fc >0.5 and <-0.5; adjusted *P*-value <0.05) suggesting a central role of the LN ecosystem in MCL transcriptional programs (Figure 1A). The 22 most differentially expressed genes (log_2Fc >5 and <-5) were predicted to belong to the extracellular region (*Online Supplementary Figure S1A*), and this was also highlighted by top functional annotations, including extracellular matrix-receptor interactions (hsa#04512), cytokines-cytokine receptor interactions (hsa#04060) and cell adhesion molecules (hsa#04514), reflecting active cellular communication between tumor cells and their ecosystems (*Online Supplementary Figure S1B*).

Because LN sections used for gene expression profiling displayed heterogeneous tumor and immune cell infiltrations, we needed to perform additional analyses to identify MCL-specific transcriptomic regulations. To this end, we compared transcriptomic data from LN with transcriptomic data from CD19$^+$ circulating MCL cells cultured on CD40L-expressing cells (Figure 1B). This *ex vivo* culture model was designed to mimic signals occurring in the LN and was composed of CD40L-expressing cells complemented by several protumoral growth factors.[13] More than 70% of the genes upregulated *ex vivo* in the culture model were also overexpressed in LN as compared with MCL PB (n=3217/4524) (Figure 1B). Accordingly, an MCL "LN signature", as well as previously described signatures enriched in MCL tissue, such as "NFκB", "BCR" or "NFκB-inducing kinase (NIK)",[15] were significantly upregulated in the *ex vivo* culture model (*Online Supplementary Figure S1C*).

By comparing the upregulated gene set (upregulated in both LN and culture, n=3,217) with CD40L-stimulated CD5$^+$ NBC, we identified that 39% of the differentially expressed genes were tumor-specific (i.e., were not upregulated in NBC) (Figure 1B). Functional annotations showed that the soluble dialog (hsa#04060) was specifically enriched in the tumor ecosystem, in contrast to extracellular matrix-receptor interactions or cell cycle activation, which were shared with NBC (*Online Supplementary Figure S1D*). Scoring of the top genes revealed that *CCL22* and *IL32* were the most upregulated genes within "Shared with NBC" and "Tumor-specific" transcriptional programs, re-

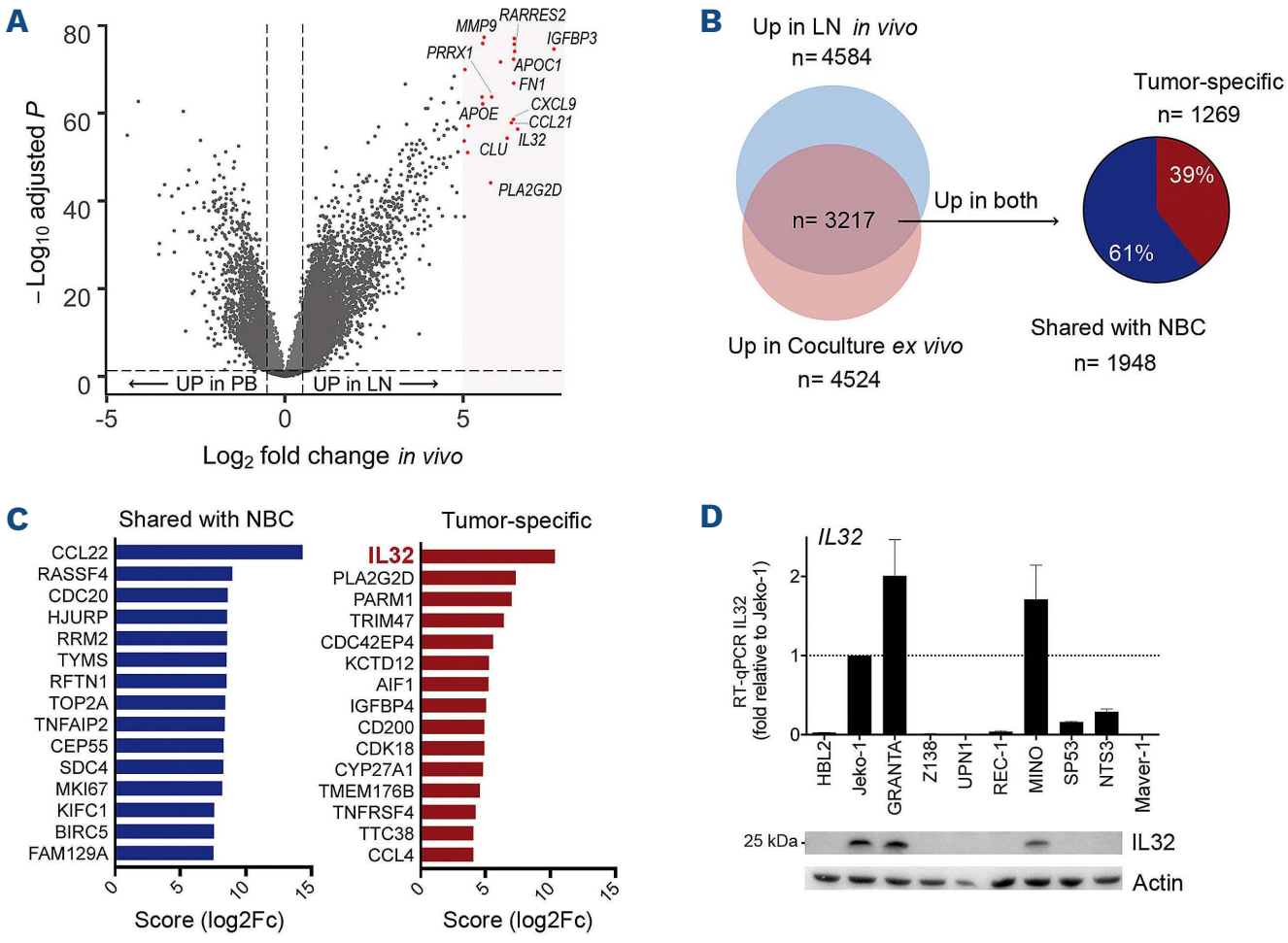

Figure 1. Microenvironment-dependent and tumor-specific IL32 expression in mantle cell lymphoma. (A) Volcano-plot representation of whole transcriptome analysis (publicly available Affimetrix U133, see Methods) from samples of mantle cell lymphoma (MCL) lymph nodes (LN, n=107) compared to MCL peripheral blood samples (PB, n=77). Dotted lines indicate the cut-off for significance (adjusted *P* value <0.05, log_2Fc >0.5 or <-0.5). The most greatly modulated genes (log_2Fc >5 or < -5) are annotated on the graph. (B) The diagram represents the comparison of the gene set induced in CD19$^+$-sorted PB MCL cultured on CD40L *ex vivo* (RNA-sequencing, see Methods) with the gene set differentially expressed between MCL LN and PB (panel A). Common *in vivo* and *ex vivo* upregulation (n=3,217 genes) were compared to the genes induced in normal CD5$^+$ B cells (NBC) cultured similarly in order to determine "Shared with NBC" and "Tumor-specific" gene sets. (C) The graphs represent the top 15 genes of "Shared with NBC" and "Tumor-specific" gene sets. The score (log_2Fc) integrates both *ex vivo* and *in vivo* modulations (log_2FC(*ex vivo*)+log_2FC(*in vivo*)). (D) IL32 expression was determined at the RNA level by quantitative reverse transcriptase polymerase chain reaction analysis (RT-qPCR, upper panel) and at the protein level (immunoblotting, lower panel) in MCL cell lines.

spectively (Figure 1C). While CCL22 production has been previously characterized as microenvironment-dependent in several B-cell malignancies,[19] the mechanisms of regulation and the biological role of IL32 have remained unknown. Constitutive expression of IL32 in three of nine cell lines first confirmed that MCL does indeed have the ability to produce and secrete IL32 (Figure 1D, *Online Supplementary Figure S2A*). Finally, splicing analysis of RNA-sequencing data showed that the predominant isoform in MCL was IL32β (*Online Supplementary Figure S2B*).

IL32 is expressed in mantle cell lymphoma lymph nodes and is induced *in vitro* upon CD40 triggering

We showed that PB MCL displayed a slight, but significant, overexpression of IL32 when compared to NBC, and high expression was observed in most LN MCL studied (Figure 2A). IL32 induction in LN was confirmed in paired samples both at the RNA (n=8) and protein (n=3) levels (Figure 2B). Consistently with our observation in cell lines, constitutive RNA expression was detected in 24% of PB MCL samples (5 out of 21), independently of p53 status or disease subtype (*Online Supplementary Table S1*). CD40L induced IL32 expression in ten out of 13 MCL samples but not in NBC (Figure 2C, D). Of note, the three samples in which IL32 induction was not detected were all from the indolent leukemic non-nodal subtypes of MCL. A similar CD40-dependent induction of IL32 was observed in MCL cell lines (*Online Supplementary Figure S2C, D*).

To further characterize the pattern of IL32 expression *in situ*, we performed immunohistochemistry on four MCL tissue samples. Figure 3A shows IL32$^+$ cells in all four of the four MCL samples. We further used multiplex immunohistochemistry in two samples for the concurrent detection of MCL cells (Cyclin D1), macrophages (CD68), T cells (CD3) and IL32. We observed that IL32 expression was enriched *in situ* in tumor zones infiltrated with T cells (ROI#1 and ROI#2 of sample LN#2, ROI#1 of sample LN#3), compared to areas containing only tumor cells (ROI#2 of LN#3) (Figure 3B, C). Taken together these results show that IL32 is expressed *in situ* by MCL cells in the vicinity of T cells.

CD40L-dependent IL32 expression in mantle cell lymphoma cells depends on the alternative NFκB pathway

We next determined whether NFκB pathways controlled IL32 induction. CD40 triggers activation of both the classical (ser32/34 IκBα phosphorylation, pIκB) and the alter-

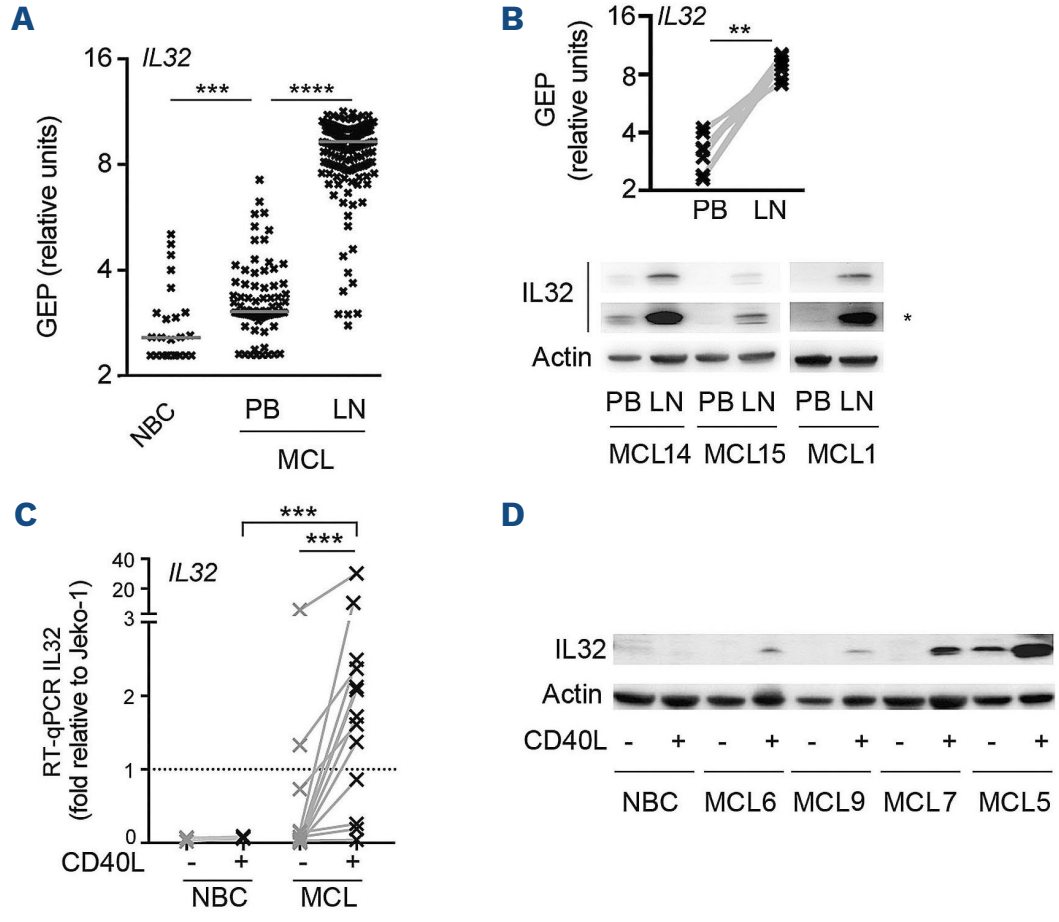

Figure 2. IL32 is expressed in mantle cell lymphoma lymph nodes and induced *in vitro* upon CD40 triggering. (A) *IL32* gene expression in normal B cells (NBC, n=24) and mantle cell lymphoma (MCL) cells from peripheral blood (PB, n=81) or lymph nodes (LN, n=165) was assessed by gene expression profiling (GEP). Mann-Whitney test. ***P<0.0005, ****P<0.0001. (B) IL32 expression was analyzed by GEP in paired MCL cells from PB (n=8) or LN (n=8) and by immunoblot in paired PB and LN tissues (frozen sections) from MCL patients (n=3). *Represents higher exposure for immunoblotting. Wilcoxon-matched pairs sign-rank test. **P<0.008 (C) Quantitative reverse transcriptase polymerase chain reaction (RT-qPCR) analysis of *IL32* gene was performed in CD5$^+$ NBC (n=3) or MCL cells (n=13) cultured on CD40L-expressing cells for 7 days. Wilcoxon-matched pairs sign-rank test. ***P<0.0005. (D) Immunoblot analysis of IL32 protein expression was performed in CD5$^+$ NBC (n=1) or MCL cells (n=4) cultured on CD40L-expressing cells for 7 days.

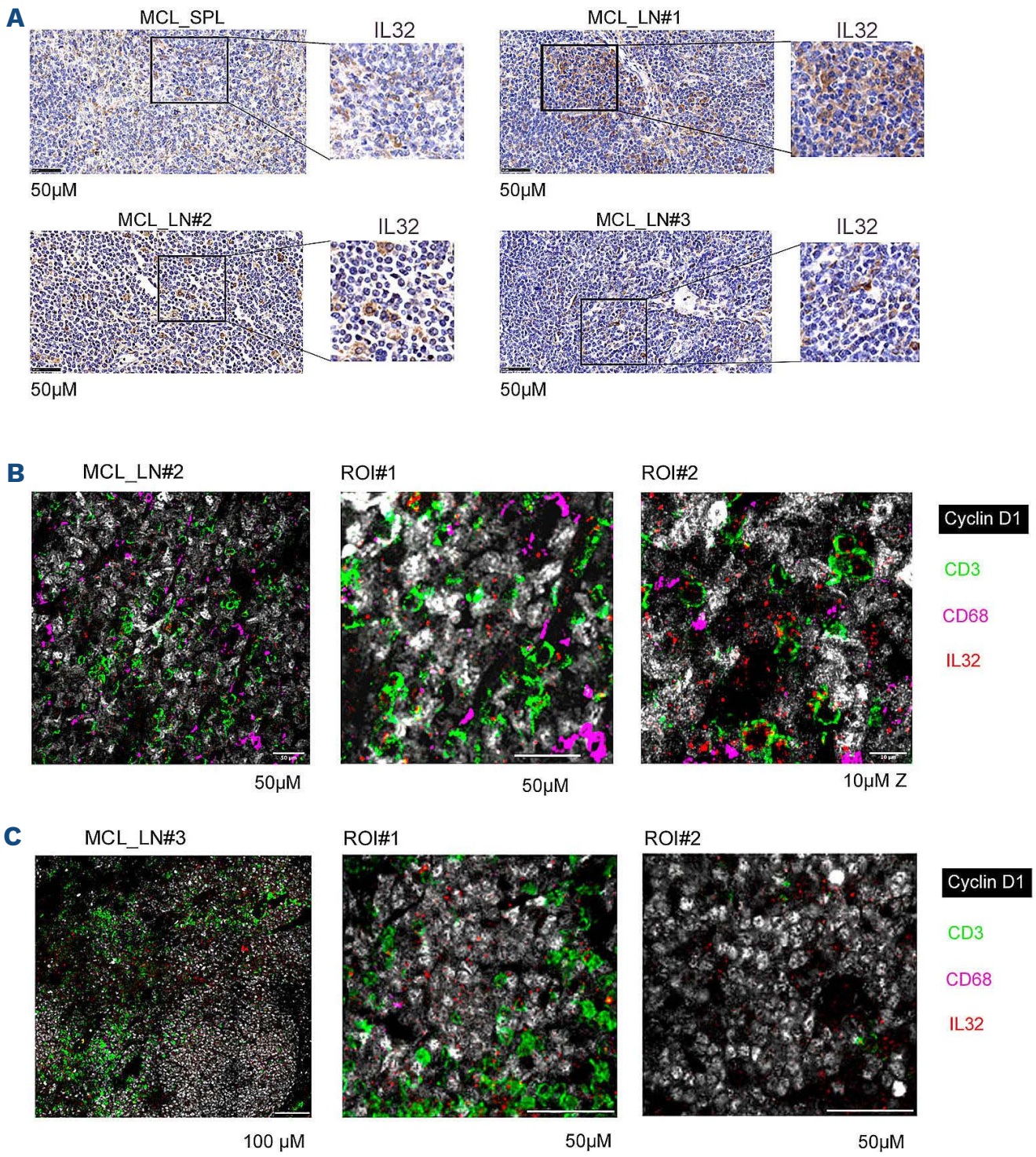

Figure 3. Protein expression of IL32 in mantle cell lymphoma lymph nodes *in situ*. (A) Expression of IL32 was determined using immunohistochemistry on one spleen (SPL) and three lymph node (LN) sections from four patients with mantle cell lymphoma (MCL). Scale bars, 50 µm. (B, C) Multiplex immunohistochemistry staining for Cyclin D1 (opal 570; white), CD3 (opal 690; green), CD68 (opal 520; magenta) and IL32 (opal 650; red) was performed on LN sections from two MCL patients (MCL_LN#2, MCL_LN#3). Individual stains and DAPI are shown in *Online Supplementary Figure S9*. For MCL-LN#2, the left panel represents a mosaic, the middle panel (region of interest, ROI#1) a zoom on the sample (scale bars, 50 µm) and the right panel (ROI#2) represents a projection of 26 Z stacks (range 10 µm; scale bar 10 µm). For MCL-LN#3, the left panel represents a large area (scale bar, 100 µm), the middle panel (ROI#1) shows a CD3-infiltrated area and the right panel (ROI#2) represents a tumor-only area (scale bars, 50 µm).

native (p52 increase) NFκB pathways (Figure 4A). Inhibition of IκB kinases IKK-1/2, using BMS-345541,[20] dramatically reduced the activation of both NFκB pathways and resulted in the complete inhibition of IL32 (*Online Supplementary Figure S3A*). However, siRNA against *NFKB1* failed to reduce IL32 expression in Mino cells (*Online Supplementary Figure S3B*), suggesting that the classical NFκB pathway was not involved. To confirm the role of the alternative pathway, we used the NIK inhibitor SMI-1, which was recently described as selectively inhibiting the alternative NFκB pathway.[21] This NIK inhibitor, which inhibited p52 processing from p100 without inducing any modulation of pIκB, resulted in the inhibition of both constitutive (Mino) and CD40L-induced (NTS3, REC1 and primary MCL) IL32 (Figure 4B,C). Of note, the detection of high p52 expression in LN tissue further confirmed the activation of an alternative NFκB pathway *in vivo* (*Online Supplementary Figure S3C*). Nevertheless, even though IL32 induction was restricted to tumor cells, activation of the alternative NFκB pathway was observed in both NBC and MCL cells upon CD40 triggering (Figure 4D). Moreover, p52 constitutive cell lines did not necessarily express IL32 (Figure

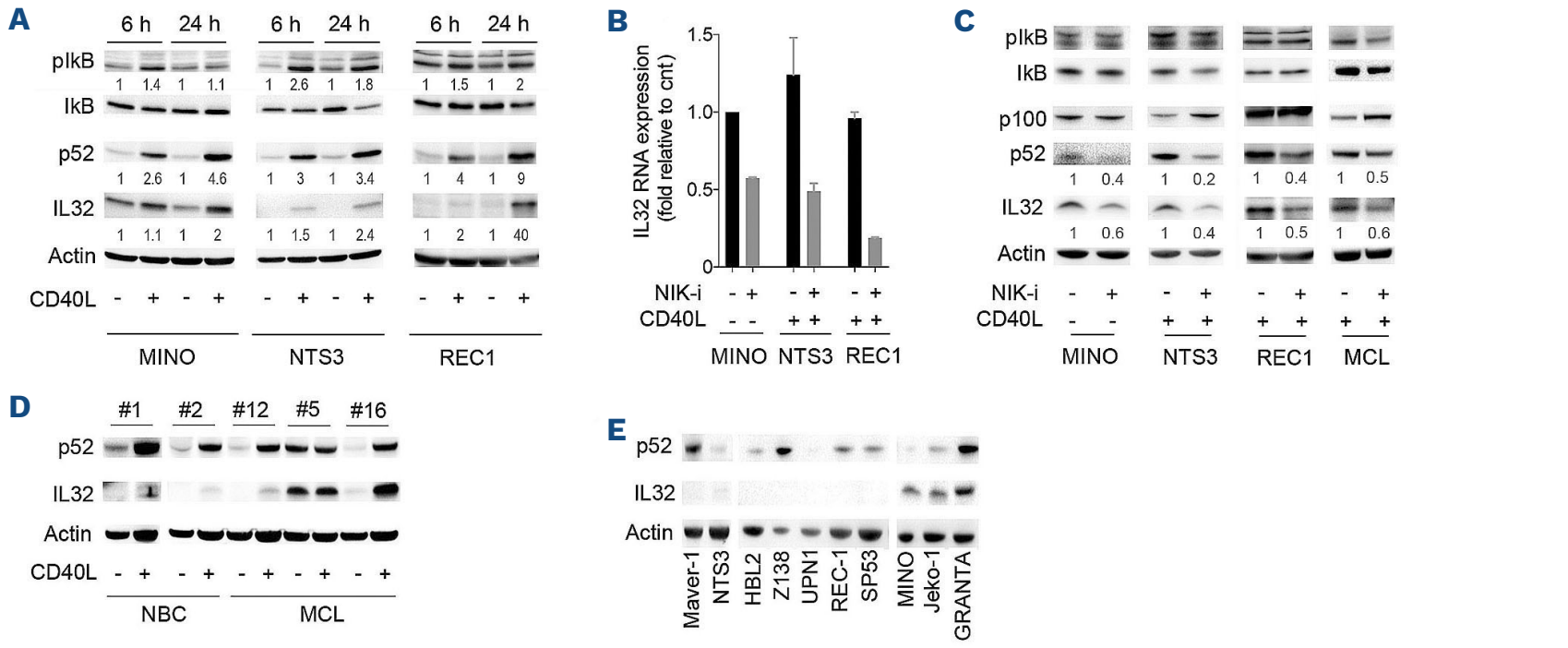

Figure 4. CD40L-dependent IL32 expression depends on the alternative NFκB signaling pathway. (A) Immunoblotting of the classical (pIκB) and alternative (p52) NF-κB pathways and IL32 protein was performed in mantle cell lymphoma (MCL) cell lines cultured on CD40L-expressing cells for the indicated time. (B, C) Quantitative reverse transcriptase polymerase chain reaction (RT-qPCR) analysis of the *IL32* gene (B) and immunoblotting of the indicated proteins (C) were performed in MCL cell lines cultured on CD40L-expressing cells for 96 h in the presence or absence of the NIK inhibitor SMI-1 (NIK-i, 10 μM). (D, E) Immunoblotting of p52 and IL32 proteins in: (D) $CD19^+CD5^+$ NBC (n=2) or $CD19^+CD5^+$ MCL cells (n=3) at day 0 and after culture on CD40L-expressing cells for 7 days and (E) MCL cell lines (n=10).

4E), suggesting that the alternative NFκB pathway may not be sufficient for IL32 induction, leading us to investigate another layer of regulation.

IL32 is hypomethylated in mantle cell lymphoma cells

We wondered whether the *IL32* locus could also be epigenetically regulated. Indeed, decitabine induced IL32 expression in IL32-negative MCL cells (*Online Supplementary Figure S4A*). Bisulfite sequencing showed that IL32-positive and negative MCL cells displayed a significantly different methylation pattern in both the promoter and CpG islands of the *IL32* gene locus (40.5% *vs*. 73% and 24% *vs*. 97%, respectively), suggesting that hypomethylation favored IL32 expression (*Online Supplementary Figure S4B*). Similarly, the IL32 promoter was hypermethylated in NBC compared to MCL cells (100% *vs*. 40.5%, respectively) and this pattern remained stable even after the NBC were stimulated with CD40L (*Online Supplementary Figure S4C, D*). Collectively our data argue for epigenetic-driven expression of IL32, explaining the tumor-restricted expression.

Myeloid cells respond strongly to IL32

We next decided to assess the biological consequences of IL32β production within the MCL ecosystem. We first addressed the role of rhIL32β on the tumor itself, but did not observe any changes, either on MCL cell survival and proliferation *ex vivo* or on previously-described IL32-induced signaling pathways and expression of protumoral factors[22] (Figure 5A, B and *data not shown*).

As the IL32 receptor has yet to be identified, we performed functional annotations of IL32 co-regulated genes within lymphoma LN to decipher the cell types that could respond to MCL-produced IL32β. We observed enrichment in pathways such as phagosome (hsa#04145), chemokine (hsa#04062) and Th17 differentiation (hsa#04659), suggesting myeloid and T-cell involvement in MCL-related IL32β functions (*Online Supplementary Figure S5A*). In addition, the top *IL32* co-regulated genes were enriched with key regulators of macrophage function as well as the T-cell-related marker CD2 (adjusted *P* value <0.0001) (*Online Supplementary Figure S5B*). Consistently, the induction of STAT3 phosphorylation on Tyr705 (pSTAT3) in both cell types confirmed the cells' ability to respond to IL32, with monocytes also displaying additional induction of NFκB pathways (Figure 5C). We next analyzed the transcriptome of rhIL32β-stimulated monocytes (Mono, n=3), monocyte-derived macrophages (Mϕ, n=3) and T cells (T, n=3). As shown in the principal component analysis, IL32β greatly modulated both monocytes and Mϕ, but only slightly the T-cell transcriptome (Figure 5D). Consistently, hierarchical clustering was able to discriminate myeloid cells according to IL32β stimulation by not T cells (Figure 5E).

We then focused on common modulations and their resulting functional annotations, arising from IL32β-stimulated monocytes and Mϕ (*Online Supplementary Figure S5C,D*). Consistent with the activation of STAT3 and NFκB pathways at the protein level (Figure 5C), we observed a significant enrichment in JAK-STAT (hsa#04630) and NF-

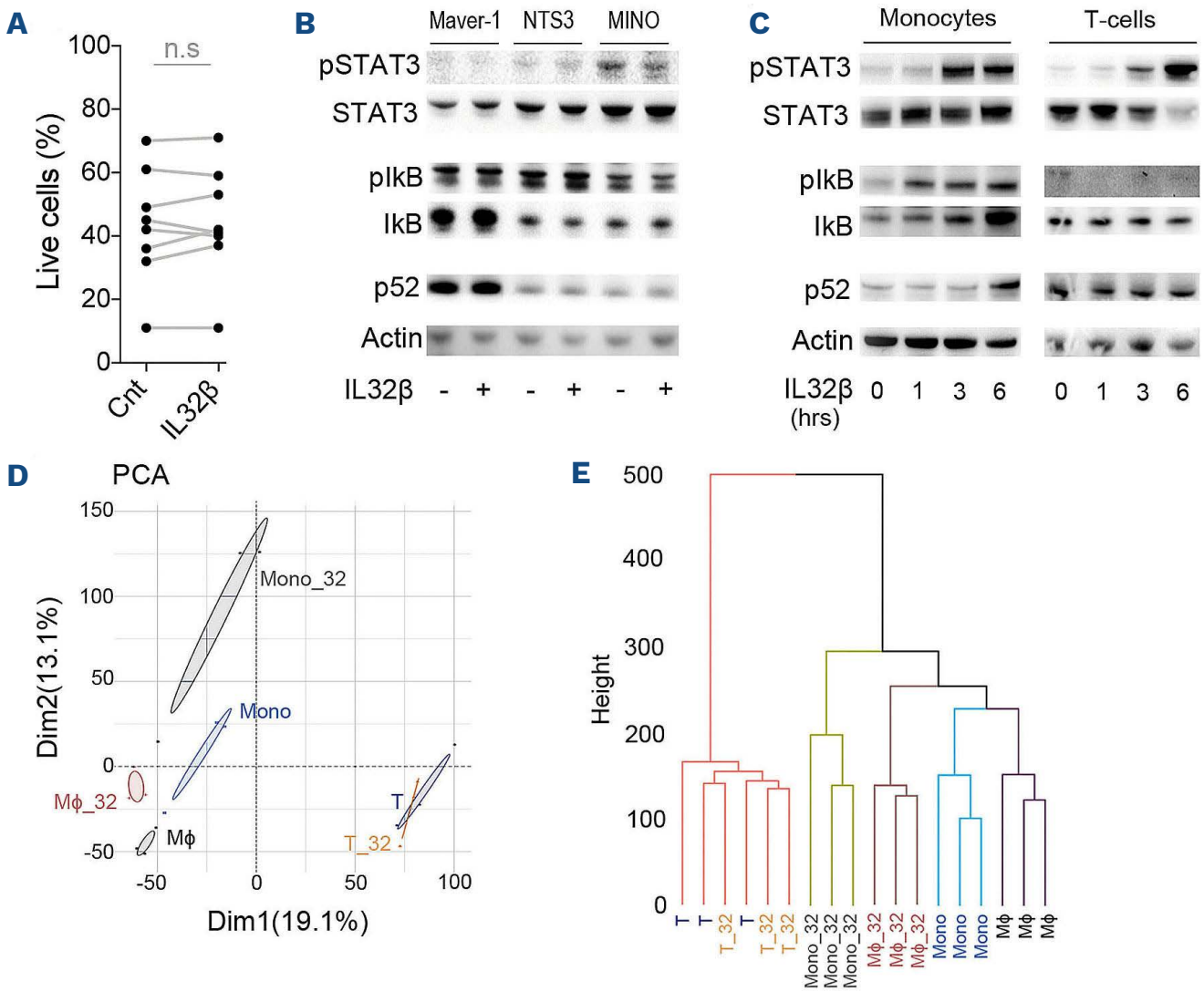

Figure 5. Myeloid cells, but not mantle cell lymphoma cells, respond to IL32β. (A) Survival of mantle cell lymphoma (MCL) cells (n=8) cultured with or without recombinant human (rh)IL32β (100 ng/mL) for 7 days was measured by lack of annexin-V staining. Wilcoxon-matched pairs sign-rank test: n.s: not significant. (B, C) Immunoblotting of the indicated proteins was performed in (B) MCL cell lines cultured with or without (rh)IL32β for 6 h or (C) $CD14^+$ monocytes and $CD3^+$ T cells isolated from healthy donors and cultured with 100 ng/mL of (rh)IL32β for the indicated times. (D) The figure represents the principal component analysis of monocytes (Mono, n=3), macrophages (Mϕ, n=3) and T cells (T, n=3) cultured for 24 h with or without 100 ng/mL of (rh)IL32β. Mϕ were first polarized with macrophage colony-stimulating factor (50 ng/mL, for 5 days) and then stimulated during 48 h with 100 ng/mL of (rh)IL32β. Colored ellipses are drawn around the mean of the group (barycenter), with the 95% confidence interval of the mean in the corresponding plan. (E) An ascendant hierarchical clustering based on 19,203 genes was constructed with the ward.D2 method of Euclidiean distances.

κB (hsa#04064) pathways (*Online Supplementary Figure S5D*). In addition, enrichment of several pathways related to soluble factors, such as IL17 (hsa#04657), TNF (hsa#04668), chemokine and cytokine signaling (hsa#04062, hsa#04060), suggested that IL32β might regulate the secretome of monocytes/Mϕ (*Online Supplementary Figure S5D*). Taken together these results suggested that IL32β secreted by MCL in its ecosystem would result in the stimulation of monocytes/Mϕ and potentially influence their secretome.

Mantle cell lymphoma-secreted IL32β led to specific differentiation of monocytes into protumoral $CD163^+$ macrophages Mϕ-32

To determine the nature of the secretome modifications in monocytes/macrophages stimulated by IL32β, we further focused our analysis on a list of 370 cytokines and chemokines (annotated in GO#0008009 and #0005125). Among them 108 were expressed in at least one sample and many of them were induced after IL32β stimulation in monocytes (n=48) or macrophages (n=40) (Figure 6A). Most of these modulations were observed in both monocytes and macrophages (n=29) and were validated by quantitative reverse transcriptase polymerase chain reaction and cytokine array (*Online Supplementary Figure S6*). To confirm these results with MCL-secreted IL32β, we generated $IL32^{-/-}$ Mino cells (*Online Supplementary Figure Figure S7A, B*) and evaluated the ability of their supernatant to induce the validated rhIL32β-modulated genes on monocyte/macrophages (*IL1A*, *IL1B*, *IL6*, *IL24*, *CXCL8*, *TNFSF13B*, and *IL32*). As expected, $IL32^{-/-}$ MINO supernatant was characterized by a lesser ability to induce these genes in monocytes/macrophages compared to $IL32^{+/+}$ cells (Figure 6B). These results were confirmed with CD40L-stimulated $IL32^{-/-}$ NTS3 cells (*Online Supplementary Figure S7C*).

Using previously published macrophage subtype characterization,[12] we determined that IL32β-induced soluble

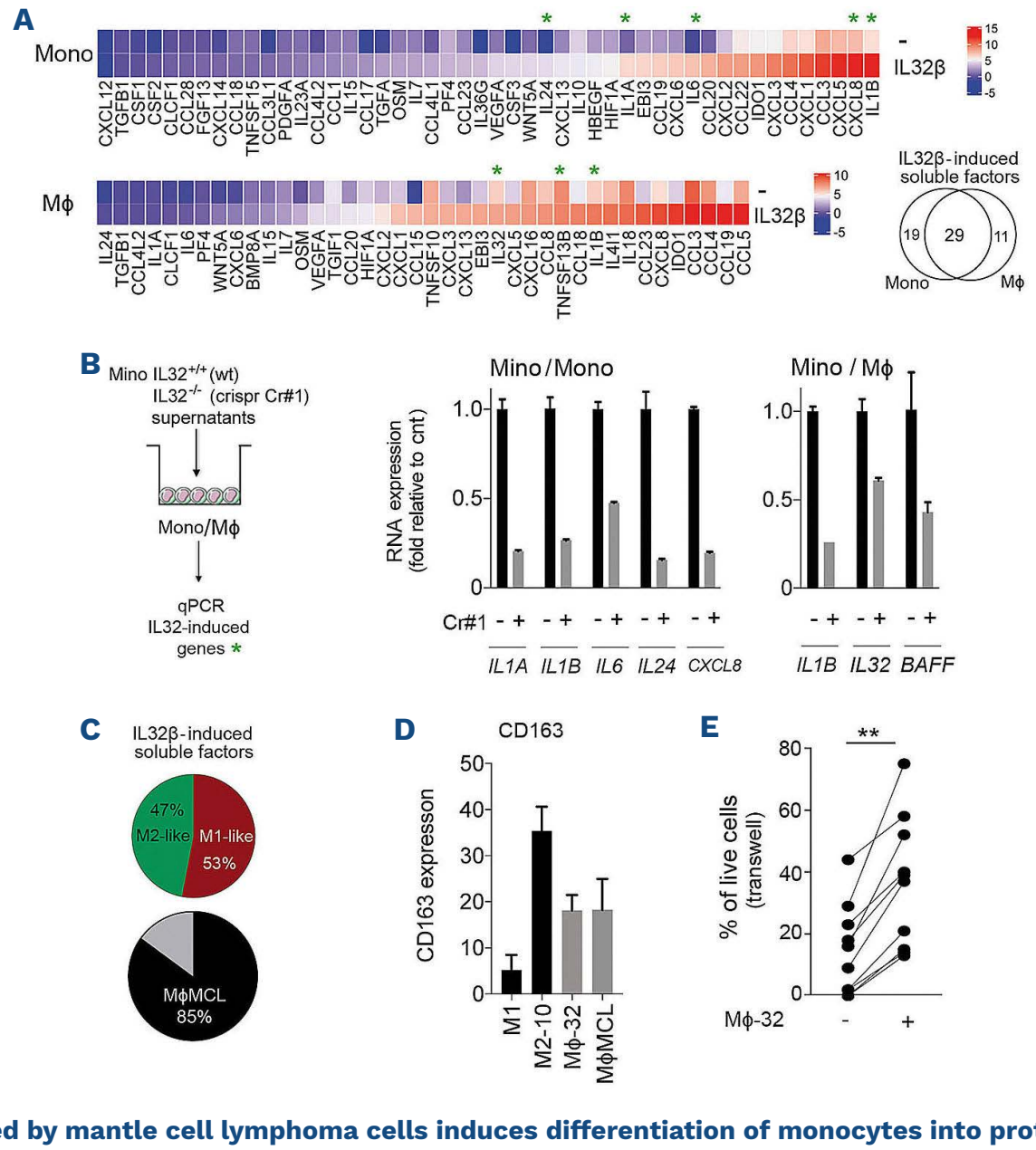

Figure 6. IL32β secreted by mantle cell lymphoma cells induces differentiation of monocytes into protumoral Mϕ-32. (A) Heatmaps of soluble factor transcripts modulated (log_2Fc >0.1) in monocytes (Mono, n=3) and monocyte-derived macrophages (Mϕ n=3) cultured with or without recombinant human (rh)IL32β as described in Figure 5D. For each cell type, the median gene expression was calculated on normalized and transformed data (DESeq2 package). The colors indicate the intensity of the median gene expression as indicated (log scale). *Indicates that gene expression was confirmed by quantitative reverse transcriptase polymerase chain reaction (RT-qPCR) as represented in *Online Supplementary Figure S6A*. (B) The left panel details the experimental protocol related to the right panel. The right panel represents RT-qPCR analysis of seven genes (*IL1A*, *IL1B*, *IL6*, *IL24*, *CXCL8*, *IL32* and *BAFF*) in Mono or Mϕ cultured, for 24 h or 48 h, respectively, with wild-type (-) or *IL32*$^{-/-}$ (Cr#1) Mino supernatant. (C) Forty-eight IL32β-induced soluble factors on Mono or Mϕ were classified as M1-like, M2-like (upper panel) or MϕMCL-like (lower panel) as previously reported.[12] (D) CD163 mean fluorescence intensity ratio was determined by flow-cytometry for M1 (n=3), M2-10 (n=4) and Mϕ32 (monocyte-derived macrophages differentiated with 50 ng/mL CSF1 for 5 days and then stimulated with 100 ng/mL rhIL32β for 48 h, n=3) and MϕMCL (monocyte-derived macrophages in the presence of MCL cells, n=3). M1, M2-10 and MϕMCL were generated as previously described.[12] (E) The percentage of MCL live cells was assessed by lack of annexin-V staining after 3 days of culture alone (-) or with Mϕ32 and separated by transwell inserts (n=10). Wilcoxon-matched pairs sign-rank test. **P<0.005.

factors were associated with both M1-like (53%) and M2-like (47%) secretomes. We recently described such a dual M1/M2 profile in MCL-associated macrophages (Mϕ-MCL) and accordingly 85% of IL32β-induced factors were found to be expressed by Mϕ-MCL (Figure 6C).[12] In addition, these macrophages (Mϕ-32) displayed similar CD163^{mid} expression, a marker of protumoral macrophages, which we previously described regarding Mϕ-MCL (Figure 6D). Finally, using culture inserts, we confirmed that the Mϕ-32 secretome was protumoral, inducing a 3-fold increase in MCL cell survival compared to that of MCL cells alone (median survival 12.5% *vs*. 38%; P<0.01) (Figure 6E).

Collectively these results showed that monocytes/macrophages responded to MCL-secreted IL32β, resulting in their polarization into protumoral CD163^{mid} Mϕ-32 expressing both an M1 and an M2-associated secretome, which was similar to that of Mϕ-MCL.

BAFF is involved in Mϕ-32 prosurvival dialog through activation of the alternative NFκB pathway in mantle cell lymphoma cells

Lastly, we aimed to discover the factors involved in the prosurvival soluble dialog between Mϕ-32 and MCL cells. We first tested a panel of nine growth factors induced by

IL32β for their capacity to support long-term (7 days) survival of MCL cells (Figure 7A). Remarkably, only BAFF was able to support MCL-cell survival alone (n=9) at a level similar to that of Mϕ-32 supernatant (s_ Mϕ-32) (Figure 7B). BAFF binds to three receptors, BAFF-R, TACI and BCMA, the last two being shared with the growth factor, A proliferation-inducing ligand (APRIL). In contrast to BAFF, APRIL did not support MCL survival (Figure 7B), suggesting that TACI and BCMA were not involved in the protumoral dialog studied here. We showed that most MCL cells highly expressed *BAFFR* and that *TNFSF13B* expression was enriched in MCL LN when compared to PB (P<0.0001), suggesting a key role of this growth factor in MCL tissue (*Online Supplementary Figure S8A, B*). We also confirmed that Mϕ-32 were able to secrete a significant amount of BAFF, in contrast to MCL (Figure 7C), and showed that rhBAFF induced the selective activation of the alternative NFκB pathway in MCL cells and cell lines (processing of p52) (*Online Supplementary Figure S8C*). Accordingly, NIK inhibition was able to counteract the survival support provided by rhBAFF in MCL cells (median reduction of 95%, n=4, P<0.05) (*Online Supplementary Figure S8D*). NIK inhibition also reduced the survival support provided by Mϕ-32 supernatant, with a median reduction of 47% (n=6, P<0.05) and almost complete reduction in three of six samples, suggesting an involvement of BAFF in Mϕ-32 supernatant (Figure 7D). Indeed, in these NIK-inhibitor-sensitive samples, BAFF-R-neutralizing antibodies resulted in the inhibition of Mϕ-32 supernatnat protumoral support with a level similar to that of the NIK inhibitor (Figure 7E). Accordingly, Mϕ-32 supernatant resulted in activation of the alternative NFκB pathway, which was counteracted using BAFF/BAFF-R-neutralizing antibodies (Figure 7F, *Online Supplementary Figure S8E*). Taken together, these data showed that BAFF secreted by Mϕ-32 was involved in the protumoral dialog with MCL, which can be counteracted by a selective NIK inhibitor or BAFF-R-neutralizing antibodies.

Discussion

IL32 is a newly characterized cytokine of which there are

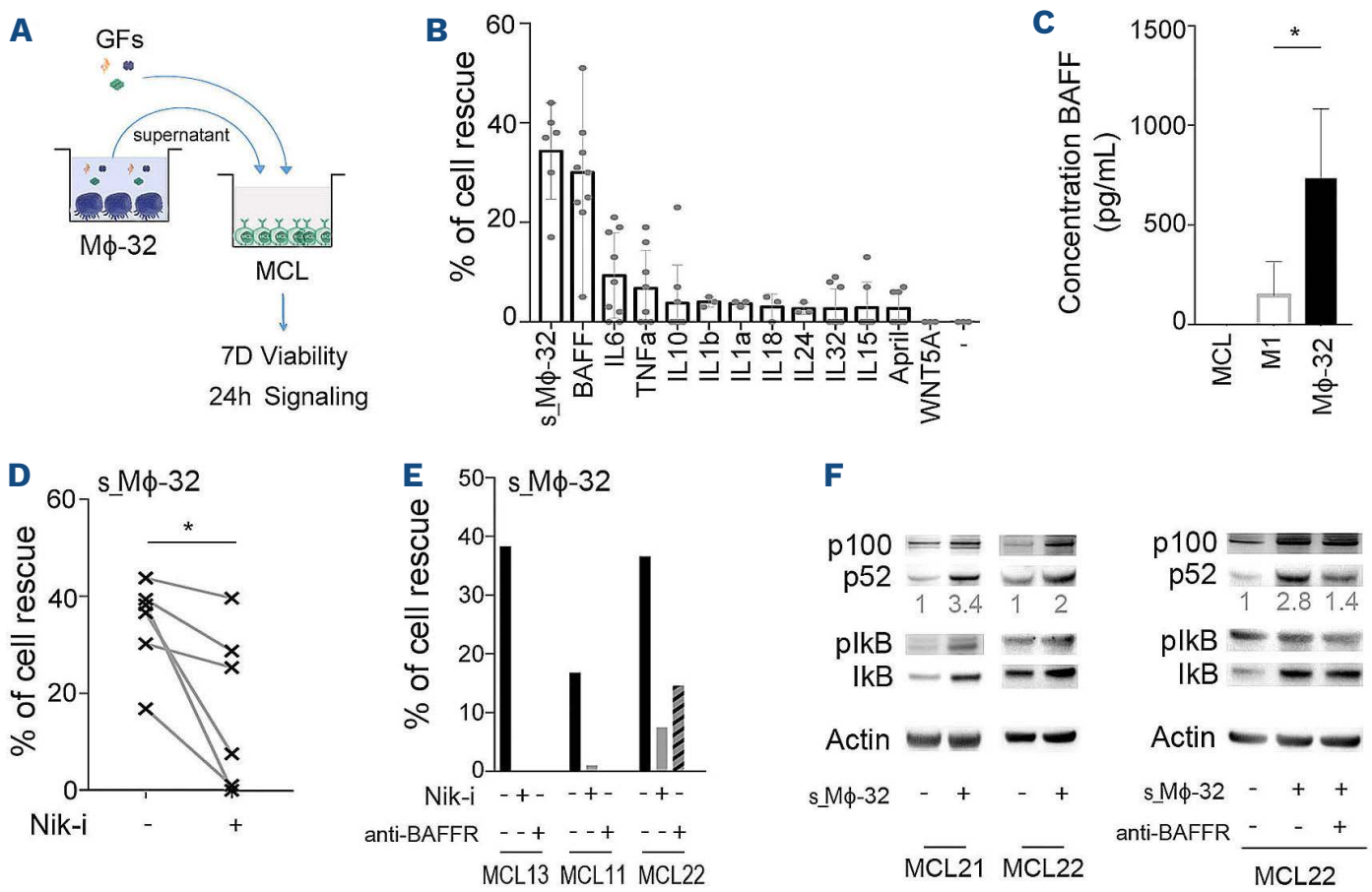

Figure 7. BAFF supports the Mϕ-32 prosurvival effect through activation of the alternative NFκB pathway. (A) Schematic representation of the protocol used. (B) Mantle cell lymphoma (MCL) cells (5x10^5 cells/mL) were cultured with macrophages polarized with IL32 supernatant (s_Mϕ-32, n=6) or growth factors: BAFF (100 ng/mL), IL6 (20 ng/mL), IL10 (100 ng/mL), IL32β (100 ng/mL), TNFα (20 ng/mL), IL15 (20 ng/mL), APRIL (100 ng/mL), IL1β (50 ng/mL), IL1α (50 ng/mL), IL24 (100 ng/mL), IL18 (50 ng/mL) and WNT5A (200 ng/mL) (n≥3). The percentage of cell rescue was assessed after 7 days of *ex vivo* culture. (C) Concentration of BAFF protein was evaluated by enzyme-linked immunosorbent assay in the supernatant of MCL cell lines (n=5), M1 (n=3) and Mϕ-32 (n=5) monocyte-derived macrophages. Unpaired *t* test. *P<0.05. (D) The percentage of cell rescue dependent on Mϕ-32 supernatant (s_Mϕ-32) in MCL cells (n=6) cultured with or without an NIK inhibitor (NIK-i, 10 μM) for 7 days was determined by annexin V staining. Paired *t* test. *P<0.05. (E) Percentage of cell rescue dependent on Mϕ-32 supernatant (s_Mϕ-32) in primary MCL (n=3) cultured with or without NIK inhibitor (NIK-i, 10 μM) or anti-BAFFR neutralizing antibody (4 μg/mL) for 7 days. (F) Immunoblotting of classical (pIκB, IκB) and alternative (p100, p52) NF-κB pathways in MCL cells cultured with Mϕ-32 supernatant (s_Mϕ-32) for 24 h with or without anti-BAFFR neutralizing antibody (4 μg/mL) as indicated.

seven variants, generated by alternative splicing, with differential biological roles.[23,24] IL32α, IL32β and IL32ɣ are the isoforms that have been studied the most up to now, with IL32β being the most frequently expressed in cancer,[25] as shown here for MCL. The putative receptor for IL32 is unknown and the lack of IL32 expression in rodents considerably limits our knowledge on its physiological roles. Nevertheless, IL32β expression has been documented in several solid cancers and this cytokine seems to be involved in many biological processes such as migration, metastasis, proliferation, and apoptosis.[25] We have shown here that IL32β, which was secreted by lymphoma cells, did not directly increase tumor cell survival, but participated in the tumor-specific shaping of macrophages. Such a paracrine role of IL32 has been recently described in multiple myeloma, a plasma cell neoplasm,[26] reinforcing the critical role of this soluble factor in the ecosystem of B-cell malignancies.

Whereas IL32 was initially characterized for its pro-inflammatory properties,[27] recent studies have highlighted that IL32 was preferentially expressed in regulatory T cells in the bone marrow[28] and that it was able to promote immunoregulatory responses, especially through the induction of IL10 or indoleamine 2, 3-dioxygenase (IDO) by macrophages.[29-31] Here we have confirmed, through a transcriptomic analysis of IL32β-induced genes in monocytes/macrophages, the ability of IL32β to induce the production of both pro-inflammatory (e.g., IL6, OSM, IL1α, and IL1β) and anti-inflammatory (e.g., IL10, IDO, IL18, IL4L1, and CCL22)[19,32,33] soluble factors (Figure 5).

We have recently published that, through a soluble interplay, MCL cells polarize monocytes into tumor-specific macrophages (Mϕ-MCL), which in turn favor tumor survival.[12] We have demonstrated that Mϕ-MCL express both pro- (M1) and anti- (M2) inflammatory associated secretomes, suggesting that factors other than classical M2-polarizing factors (such as MCL-secreted IL10 and CSF-1) might be involved in the Mϕ-MCL phenotype. Herein, we have shown that MCL-secreted IL32β is most likely to be involved in this specific MCL-associated macrophage profile, with most of these M1 and M2-like factors being common to both Mϕ-MCL and Mϕ-32. In addition, Mϕ-32 share Mϕ-MCL phenotypic and functional characteristics i.e., $CD163^{mid}$ expression or MCL survival support through soluble dialog, respectively (Figure 6). Only a few studies have addressed the crosstalk between tumor-associated macrophages and MCL cells, so far.[12,34,35] Of note, a recent publication highlighted that LN infiltrating $CD163^{+}$ MCL-associated macrophages correlate with a poor prognosis in MCL,[36] suggesting that targeting this interplay could be an interesting perspective for novel therapeutic options.

Of the various IL32β-induced secretomes, several have been previously described as being involved in MCL expansion, such as IL6, IL10, BAFF and WNT5A.[37-40] Nevertheless, we have shown that only BAFF supported the long-term survival of MCL cells alone, at a level similar to that observed with the Mϕ-32 supernatant. Although BAFF is a well-described survival and growth factor for both normal and malignant B cells,[39] only a few publications have addressed the functional consequences of BAFF stimulation in MCL.[41] We have shown that most MCL samples express BAFF-R, and its activation leads to selective processing of the alternative NFκB pathway (Figure 7). Of note, Medina and colleagues previously demonstrated that mesenchymal stem cell-dependent MCL survival was also mediated by BAFF, suggesting a central role for this growth factor in MCL ecosystems.[42] Neutralizing antibodies are available for targeting either BAFF (belimumab) or BAFF-R (VAY-736), both of which display interesting preclinical activity, alone or in combination with BTK inhibitors, in B-cell malignancies such as chronic lymphocytic leukemia.[43,44]

Our results highlight a major role of the alternative NFκB pathway in the interplay between CD40-activated MCL cells and macrophages, especially through the IL32/BAFF axis. Saba and colleagues highlighted that a so-called "NIK signature", reflecting the activity of the alternative NFκB pathway, was enriched in MCL LN tissue compared to PB.[15] Consistent with these results, we previously demonstrated strong processing of p52 in our CD40L culture model designed to mimic signals occurring within the LN.[13] Here we have confirmed that MCL cells cultured in this model are also characterized by the NIK signature (*Online Supplementary Figure S1*). The alternative NFκB pathway is frequently constitutively activated in MCL by intrinsic anomalies in several key elements of this pathway, such as *MAP3K14* (coding for NIK), *TRAF2*, *BIRC3* and *TRAF3*.[45] In the present work, we have shown that activation of the alternative NFκB pathway is also able to influence the MCL ecosystem through microenvironment-dependent and tumor-specific IL32 induction and consecutive macrophage (re)programming. Thus, the alternative NFκB pathway activation can be the consequence of both intrinsic anomalies and microenvironment interactions, highlighting a central role of this pathway, which appeared to be involved in drug resistance. Indeed, Rahal and colleagues showed that its constitutive activity was involved in resistance to ibrutinib in MCL cell lines.[11]

We previously demonstrated that CD40L-dependent survival was associated with an NFκB-dependent imbalance of the BCL-2 family in MCL, including dramatic induction of anti-apoptotic proteins such as BCLxL.[13,14] Even though BAFF is a well-described pro-survival factor, the precise molecular mechanisms involved in BAFF-dependent survival remain elusive and cell-type dependent[4,6,47] In contrast to CD40L, BAFF did not induce BCLxL or MCL1 in MCL cells and only a transitory increase of BCL2A1 was detected in cell lines (*Online Supplementary Figure S8F-*

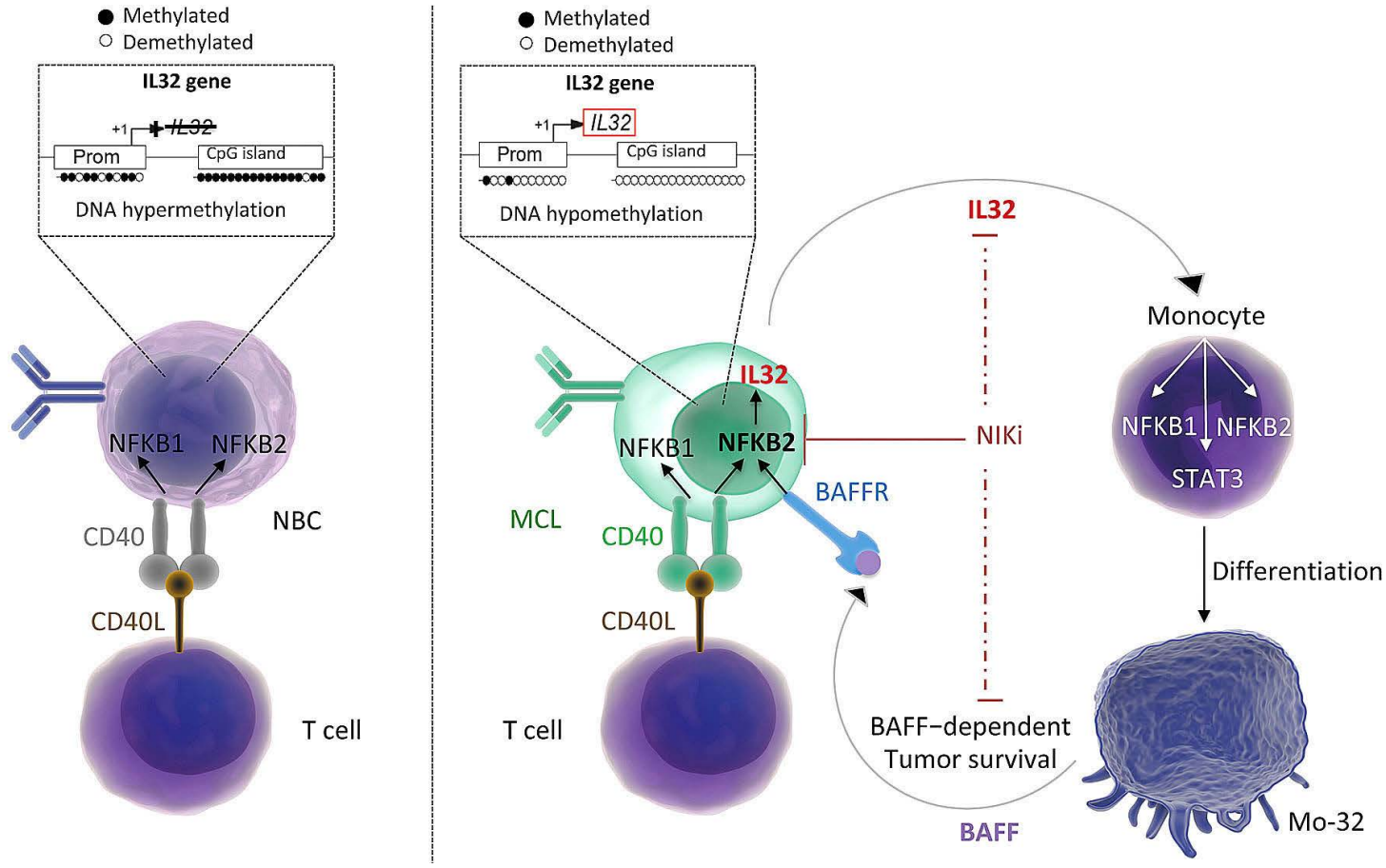

Figure 8. The IL32/BAFF axis supports prosurvival dialogs in the lymphoma ecosystem and is disrupted by NIK inhibition. Interactions between tumor cells and T cells, through the CD40-CD40L axis, result in activation of the NFκB pathways (NFκB1/2) and in NFκB2-dependent secretion of IL32 by tumor cells within their ecosystem. IL32 promoter is hypomethylated in mantle cell lymphoma (MCL) cells compared to normal B cells (NBC) resulting in tumor-restricted IL32 expression. The latter is involved in monocyte differentiation into lymphoma-associated CD163$^+$ macrophages (Mϕ-32). Mϕ-32 are characterized by a specific secretome, which includes BAFF, and supports BAFF-R/NFκB2-dependent tumoral survival. Selective NIK inhibition counteracts NFκB2 activation and consequently prevents both IL32 secretion by MCL cells and BAFF-dependent MCL-survival.

H). Taken together, our data suggest that complementary protumoral pathways occur within the ecosystem. Further studies, such as modulations of BCL2-family complexes at the mitochondrial level and characterization of mitochondrial priming upon BAFF stimulation, are now necessary to decipher the molecular mechanisms involved in BAFF/NFκB2 dependent regulation of apoptosis in MCL.

The specific inhibition of the alternative NFκB pathway was barely achievable until the very recent development of specific NIK inhibitors.[21,48] NIK is a kinase selectively involved in the alternative pathway by activating IκKα, which in turn induces the cleavage of p100 to p52, without affecting the canonical pathway. Here, we have confirmed the efficacy of NIK inhibition in counteracting microenvironment-dependent induction of IL32 (Figure 4) and BAFF-dependent survival of MCL cells (Figure 7). The central role of the NFκB pathways in mature B-cell malignancies is well-documented,[49,50] reinforcing the strong rationale to specifically target this pathway. Further development of molecules that selectively target key elements of the alternative NFκB pathway (e.g., NIK and RELB) as well as their evaluation in early phase clinical trials are now needed to address their potential therapeutic value.

In summary, our data reveal the involvement of the IL32β/BAFF axis in MCL-associated macrophage polarization and tumor survival. Our data show that targeting IL32β, BAFF or the alternative NFκB pathway could be of major interest for counteracting the multiple cross-talk that occurs in the MCL microenvironment and, especially, the CD40L$^+$ T-cell/MCL/CD163$^+$ MCL-associated macrophage triad (Figure 8).

Disclosures

No conflicts of interest to disclose.

Contributions

SD and AP designed and performed the experiments and analyzed data. CB performed experiments and participated in bioinformatics. CS, CD, TR, AMA and YLB performed experiments and analyzed data. BT and MR participated in the bioinformatics analysis. SB and PH participated in immunohistochemistry experiments and analysis. SLG participated in the design of the study. CPD participated in the design of the study, in the data analysis, and in writing the article. DC designed the study, performed experiments, analyzed data, and wrote the article.

Acknowledgments

The authors thank la Ligue Contre le Cancer Grand-Ouest,

i-Site NexT (ANR-16-IDEX-0007), the SIRIC ILIAD (INCa-DGOS-Inserm_12558), ERRATA (Région Pays de la Loire program 2015-2018) and Actions Cancer 44. CS is the recipient of a fellowship from Plan Cancer (FRFT). MicroPICell facility is a member of the national infrastructure France-BioImaging supported by the French National Research Agency (ANR-10-INBS-04). The authors thank Dr. Martine Amiot for her critical review of the manuscript. The authors are also most grateful to the Genomics and Bioinformatics Core Facility of Nantes (GenoBiRD, Biogenouest, IFB) and the flow cytometry core facility (Cytocell, SFR Bonamy) for their technical support.

Data-sharing statement

RNA-sequencing datasets are publicly available in the Gene Expression Omnibus. All other datasets analyzed during the current study are available from the corresponding author on reasonable request.

References

1. Maman S, Witz IP. A history of exploring cancer in context. Nat Rev Cancer. 2018;18(6):359-376.
2. Jin M-Z, Jin W-L. The updated landscape of tumor microenvironment and drug repurposing. Signal Transduct Target Ther. 2020;5(1):1-16.
3. Le Gouill S, Morschhauser F, Chiron D, et al. Ibrutinib, obinutuzumab and venetoclax in relapsed and untreated patients with mantle-cell lymphoma, a phase I/II trial. Blood. 2020;137(7):877.
4. Pytlik R, Polgarova K, Karolova J, Klener P. Current immunotherapy approaches in non-Hodgkin lymphomas. Vaccines. 2020;8(4):708.
5. Campo E, Rule S. Mantle cell lymphoma: evolving management strategies. Blood. 2015;125(1):48-55.
6. Delfau-Larue M-H, Klapper W, Berger F, et al. High-dose cytarabine does not overcome the adverse prognostic value of CDKN2A and TP53 deletions in mantle cell lymphoma. Blood. 2015;126(5):604-611.
7. Eskelund CW, Dahl C, Hansen JW, et al. TP53 mutations identify younger mantle cell lymphoma patients who do not benefit from intensive chemoimmunotherapy. Blood. 2017;130(17):1903-1910.
8. Nadeu F, Martin-Garcia D, Clot G, et al. Genomic and epigenomic insights into the origin, pathogenesis, and clinical behavior of mantle cell lymphoma subtypes. Blood. 2020;136(12):1419-1432.
9. Agarwal R, Chan Y-C, Tam CS, et al. Dynamic molecular monitoring reveals that SWI–SNF mutations mediate resistance to ibrutinib plus venetoclax in mantle cell lymphoma. Nat Med. 2019;25(1):119-129.
10. Chiron D, Di Liberto M, Martin P, et al. Cell-cycle reprogramming for PI3K inhibition overrides a relapse-specific C481S BTK mutation revealed by longitudinal functional genomics in mantle cell lymphoma. Cancer Discov. 2014;4(9):1022-1035.
11. Rahal R, Frick M, Romero R, et al. Pharmacological and genomic profiling identifies NF-κB–targeted treatment strategies for mantle cell lymphoma. Nat Med. 2014;20(1):87-92.
12. Papin A, Tessoulin B, Bellanger C, et al. CSF1R and BTK inhibitions as novel strategies to disrupt the dialog between mantle cell lymphoma and macrophages. Leukemia. 2019;33(10):2442-2453.
13. Chiron D, Bellanger C, Papin A, et al. Rational targeted therapies to overcome microenvironment-dependent expansion of mantle cell lymphoma. Blood. 2016;128(24):2808-2818.
14. Tessoulin B, Papin A, Gomez-Bougie P, et al. BCL2-family dysregulation in B-cell malignancies: from gene expression regulation to a targeted therapy biomarker. Front Oncol. 2018;8:645.
15. Saba NS, Liu D, Herman SE, et al. Pathogenic role of B-cell receptor signaling and canonical NF-κB activation in mantle cell lymphoma. Blood. 2016;128(1):82-92.
16. Ferrer A, Salaverria I, Bosch F, et al. Leukemic involvement is a common feature in mantle cell lymphoma. Cancer. 2007;109(12):2473-2480.
17. Hanf M, Chiron D, de Visme S, et al. The REFRACT-LYMA cohort study: a French observational prospective cohort study of patients with mantle cell lymphoma. BMC Cancer. 2016;16(1):802.
18. Charpentier E, Cornec M, Dumont S, et al. 3'RNA sequencing for robust and low-cost gene expression profiling. 2021 Jan 15: https://doi.org/10.21203/rs.3.pex-1336/v1 [preprint, not peer-reviewed].
19. Rawal S, Chu F, Zhang M, et al. Cross talk between follicular Th cells and tumor cells in human follicular lymphoma promotes immune evasion in the tumor microenvironment. J Immunol. 2013;190(12):6681-6693.
20. Burke JR, Pattoli MA, Gregor KR, et al. BMS-345541 is a highly selective inhibitor of IκB kinase that binds at an allosteric site of the enzyme and blocks NF-κB-dependent transcription in mice. J Biol Chem. 2003;278(3):1450-1456.
21. Brightbill HD, Suto E, Blaquiere N, et al. NF-κB inducing kinase is a therapeutic target for systemic lupus erythematosus. Nat Commun. 2018;9(1):1-14.
22. Sloot YJ, Smit JW, Joosten LA, Netea-Maier RT. Insights into the role of IL-32 in cancer. Semin Immunol. 2018;38:24-32.
23. Aass KR, Kastnes MH, Standal T. Molecular interactions and functions of IL-32. J Leuk Biol. 2021;109(1):143-159.
24. Sohn DH, Nguyen TT, Kim S, et al. Structural characteristics of seven IL-32 variants. Immune Netw. 2019;19(2):e8.
25. Han S, Yang Y. Interleukin-32: frenemy in cancer? BMB Rep. 2019;52(3):165.
26. Zahoor M, Westhrin M, Aass KR, et al. Hypoxia promotes IL-32 expression in myeloma cells, and high expression is associated with poor survival and bone loss. Blood Adv. 2017;1(27):2656-2666.
27. Kim S-H, Han S-Y, Azam T, Yoon D-Y, Dinarello CA. Interleukin-32: a cytokine and inducer of TNFα. Immunity. 2005;22(1):131-142.
28. Zavidij O, Haradhvala NJ, Mouhieddine TH, et al. Single-cell RNA sequencing reveals compromised immune microenvironment in precursor stages of multiple myeloma. Nat Cancer. 2020;1(5):493-506.
29. Kang JW, Choi SC, Cho MC, et al. A proinflammatory cytokine interleukin-32β promotes the production of an anti-inflammatory cytokine interleukin-10. Immunology. 2009;128(1pt2):e532-e540.

30. Smith AJ, Toledo CM, Wietgrefe SW, et al. The immunosuppressive role of IL-32 in lymphatic tissue during HIV-1 infection. J Immunol. 2011;186(11):6576-6584.
31. Yan H, Dong M, Liu X, et al. Multiple myeloma cell-derived IL-32γ increases the immunosuppressive function of macrophages by promoting indoleamine 2, 3-dioxygenase (IDO) expression. Cancer Lett. 2019;446:38-48.
32. Carbonnelle-Puscian A, Copie-Bergman C, Baia M, et al. The novel immunosuppressive enzyme IL4I1 is expressed by neoplastic cells of several B-cell lymphomas and by tumor-associated macrophages. Leukemia. 2009;23(5):952-960.
33. Nakamura K, Kassem S, Cleynen A, et al. Dysregulated IL-18 is a key driver of immunosuppression and a possible therapeutic target in the multiple myeloma microenvironment. Cancer Cell. 2018;33(4):634-648.
34. Song K, Herzog BH, Sheng M, et al. Lenalidomide inhibits lymphangiogenesis in preclinical models of mantle cell lymphoma. Cancer Res. 2013;73(24):7254-7264.
35. Le K, Sun J, Khawaja H, et al. Mantle cell lymphoma polarizes tumor-associated macrophages into M2-like macrophages, which in turn promote tumorigenesis. Blood Adv. 2021;5(14):2863-2878.
36. Rodrigues JM, Nikkarinen A, Hollander P, et al. Infiltration of CD163-, PD-L1- and FoxP3-positive cells adversely affects outcome in patients with mantle cell lymphoma independent of established risk factors. Br J Haematol. 2021;193(3):520-531.
37. Baran-Marszak F, Boukhiar M, Harel S, et al. Constitutive and B-cell receptor-induced activation of STAT3 are important signaling pathways targeted by bortezomib in leukemic mantle cell lymphoma. Haematologica. 2010;95(11):1865.
38. Karvonen H, Chiron D, Niininen W, et al. Crosstalk between ROR1 and BCR pathways defines novel treatment strategies in mantle cell lymphoma. Blood Adv. 2017;1(24):2257-2268.
39. Yang S, Li J-Y, Xu W. Role of BAFF/BAFF-R axis in B-cell non-Hodgkin lymphoma. Crit Rev Oncol Hematol. 2014;91(2):113-122.
40. Zhang L, Yang J, Qian J, et al. Role of the microenvironment in mantle cell lymphoma: IL-6 is an important survival factor for the tumor cells. Blood. 2012;120(18):3783-3792.
41. Novak AJ, Grote DM, Stenson M, et al. Expression of BLyS and its receptors in B-cell non-Hodgkin lymphoma: correlation with disease activity and patient outcome. Blood. 2004;104(8):2247-2253.
42. Medina DJ, Goodell L, Glod J, Gélinas C, Rabson AB, Strair RK. Mesenchymal stromal cells protect mantle cell lymphoma cells from spontaneous and drug-induced apoptosis through secretion of B-cell activating factor and activation of the canonical and non-canonical nuclear factor κB pathways. Haematologica. 2012;97(8):1255-1263.
43. McWilliams EM, Lucas CR, Chen T, et al. Anti–BAFF-R antibody VAY-736 demonstrates promising preclinical activity in CLL and enhances effectiveness of ibrutinib. Blood Adv. 2019;3(3):447-460.
44. Tandler C, Schmidt M, Heitmann JS, et al. Neutralization of B-cell activating factor (BAFF) by belimumab reinforces small molecule inhibitor treatment in chronic lymphocytic leukemia. Cancers. 2020;12(10):2725.
45. Hill HA, Qi X, Jain P, et al. Genetic mutations and features of mantle cell lymphoma: a systematic review and meta-analysis. Blood Adv. 2020;4(13):2927-2938.
46. Hatada EN, Do RK, Orlofsky A, et al. NF-κB1 p50 is required for BLyS attenuation of apoptosis but dispensable for processing of NF-κB2 p100 to p52 in quiescent mature B cells. J Immunol. 2003;171(2):761-768.
47. Paiva C, Rowland TA, Sreekantham B, et al. SYK inhibition thwarts the BAFF-B-cell receptor crosstalk and thereby antagonizes Mcl-1 in chronic lymphocytic leukemia. Haematologica. 2017;102(11):1890.
48. Mondragón L, Mhaidly R, De Donatis GM, et al. GAPDH overexpression in the T cell lineage promotes angioimmunoblastic T cell lymphoma through an NF-κB-dependent mechanism. Cancer Cell. 2019;36(3):268-287.
49. Kennedy R, Klein U. Aberrant activation of NF-κB signalling in aggressive lymphoid malignancies. Cells. 2018;7(11):189.
50. Eluard B, Nuan-Aliman S, Faumont N, et al. The alternative RelB NF-κB subunit is a novel critical player in diffuse large B-cell lymphoma. Blood. 2022;139(3):384-398.